Anal. Chem. **2009,** *81,* 3143–3150

Nanoscale Imaging of Surface Topography and Reactivity with the Scanning Electrochemical Microscope

François O. Laforge,† Jeyavel Velmurugan, Yixian Wang, and Michael V. Mirkin*

Department of Chemistry and Biochemistry, Queens College−City University of New York, Flushing, New York 11367

Over the last 2 decades, scanning electrochemical microscopy (SECM) has been extensively employed for topographic imaging and mapping surface reactivity on the micrometer scale. We used flat, polished nanoelectrodes as SECM tips to carry out feedback mode imaging of various substrates with nanoscale resolution. Constant-height and constant-current images of plastic and Au compact disc surfaces and more complicated objects (computer chips and wafers) were obtained. The possibility of simultaneous imaging of surface topography and electrochemical reactivity was demonstrated. Very fast mass transfer at nanoelectrodes allowed us to obtain high-quality electrochemical images in viscous media under steady-state conditions, e.g., in 1-methyl-3-octylimidazolium-bis(tetrafluoromethylsulfonyl)imide ($C_8mimC_1C_1N$) ionic liquid. Ion-transfer-based imaging was also performed using nanopipets as SECM tips.

The capacity for acquiring spatially resolved chemical information makes the scanning electrochemical microscope (SECM) a powerful tool for visualizing microstructures and studying surface processes.[1] A wide range of the reported applications include mapping local heterogeneous kinetics,[2] rapid screening of electrocatalysts,[3] studies of charge-transfer processes at liquid interfaces[1,4] and in biological cells,[5] and investigations of corrosion[6] and crystal dissolution.[7] Various substrates from enzyme-patterned molecular films[8] to diamond electrodes[9] and semiconductor surfaces[10] to living cells[11] have been imaged by SECM. Among most recent applications are visualization of one-dimensional (1-D) conductors,[12] proteins,[13] and fingerprints on surfaces.[14]

Among several modes of the SECM operation, the feedback mode offers important advantages for topographic and reaction rate imaging.[1] These include high spatial resolution due to the minimal diffusional broadening of the image and high sensitivity to the surface reactivity. Feedback mode SECM images are obtained by scanning the tip above the substrate and recording the variations in the tip current (constant-height mode) or *z*-coordinate (constant-current mode) in solution containing either oxidized or reduced form of a redox mediator. The tip current is produced by reduction (or oxidation) of the mediator species at its surface. If the mediator species is regenerated at the conductive substrate surface at the diffusion-controlled rate, such a process produces an enhancement in the tip current (positive feedback). In the absence of the mediator regeneration, an insulating substrate blocks the diffusion of redox species to the tip, and so the tip current (i_T) decreases with decreasing separation distance, d (negative feedback). The strong i_T versus d dependence under both positive and negative feedback conditions constitutes the basis for topographic SECM imaging. If the mediator regeneration at the substrate is kinetically controlled, a feedback mode SECM image provides information on the spatial distribution of the reaction rate at the substrate.[15a]

Most SECM images reported in the literature were obtained with micrometer-size tips and, therefore, provided micrometer-scale resolution.[1,16] The previously available nanotips were shaped either as a cone or a spherical cap.[17] Conical and spherical tips have been employed for generation/collection mode imaging,[18]

* To whom correspondence should be addressed. E-mail: mmirkin@qc.cuny.edu.

† Present address: Department of Chemistry, Princeton University, Princeton, NJ 08544-1009.

(1) (a) Amemiya, S.; Bard, A. J.; Fan, F.-R. F.; Mirkin, M. V.; Unwin, P. R. *Annu. Rev. Anal. Chem.* **2008**, *1*, 95. (b) Laforge, F. O.; Sun, P.; Mirkin, M. V. In *Advances in Chemical Physics*; Rice, S. A., Ed.; Wiley & Sons, 2008; Vol. 139, p 177.

(2) Wittstock, G.; Burchardt, M.; Pust, S. E.; Shen, Y.; Zhao, C. *Angew. Chem., Int. Ed.* **2007**, *46*, 1584.

(3) Fernandez, J. L.; Walsh, D. A.; Bard, A. J. *J. Am. Chem. Soc.* **2005**, *127*, 357.

(4) (a) Barker, A. L.; Gonsalves, M.; Macpherson, J. V.; Slevin, C. J.; Unwin, P. R. *Anal. Chim. Acta* **1999**, *385*, 223. (b) Mirkin, M. V.; Tsionsky, M. In *Scanning Electrochemical Microscopy*; Bard, A. J., Mirkin, M. V., Eds.; Marcel Dekker: New York, 2001; p 299.

(5) Amemiya, S.; Guo, J.; Xiong, H.; Gross, D. A. *Anal. Bioanal. Chem.* **2006**, *386*, 458.

(6) (a) Casillas, N.; Charlebois, S.; Smyrl, W. H.; White, H. S. *J. Electrochem. Soc.* **1993**, *140*, L142. (b) Wipf, D. O. *Colloids Surf., A* **1994**, *93*, 251.

(7) Macpherson, J. V.; Unwin, P. R. In *Scanning Electrochemical Microscopy*; Bard, A. J., Mirkin, M. V., Eds.; Marcel Dekker: New York, 2001; p 521.

(8) Wittstock, G.; Schuhmann, W. *Anal. Chem.* **1997**, *69*, 5059.

(9) Wilson, N. R.; Clewes, S. L.; Newton, M. E.; Unwin, P. R.; Macpherson, J. V. *J. Phys. Chem. B* **2006**, *110*, 5639.

(10) Zhu, R.; Nowierski, C.; Ding, Z.; Noeel, J. J.; Shoesmith, D. W. *Chem. Mater.* **2007**, *19*, 2533.

(11) Sun, P.; Laforge, F. O.; Abeyweera, T. P.; Rotenberg, S. A.; Carpino, J.; Mirkin, M. V. *Proc. Natl. Acad. Sci. U.S.A.* **2008**, *105*, 443.

(12) Xiong, H.; Gross, D. A.; Guo, J.; Amemiya, S. *Anal. Chem.* **2006**, *78*, 1946.

(13) Zhang, M.; Wittstock, G.; Shao, Y.; Girault, H. H. *Anal. Chem.* **2007**, *79*, 4833.

(14) Zhang, M.; Girault, H. H. *Electrochem. Commun.* **2007**, *9*, 1778.

(15) (a) Wipf, D. O.; Bard, A. J. *J. Electrochem. Soc.* **1991**, *138*, L4. (b) Wipf, D. O.; Bard, A. J. *Anal. Chem.* **1992**, *64*, 1362.

(16) Fan, F.-R. F. In *Scanning Electrochemical Microscopy*; Bard, A. J., Mirkin, M. V., Eds.; Marcel Dekker: New York, 2001; p 111.

10.1021/ac900335c CCC: $40.75
Published on Web 03/12/2009

imaging "in humid air",[16,19] and for electrochemical imaging with combined SECM−AFM (atomic force microscopy),[20] but low feedback responses make them less suitable for the feedback mode experiments. Here, we report the use of polishable disk-type nanotips[21a] for feedback mode imaging of substrate topography and reactivity. Similar probes have recently been employed for nanoscale imaging of biological cells.[11] However, it was difficult to interpret such images and evaluate their validity. In this work, the spatial resolution and other aspects of nanoscale SECM experiments will be explored by imaging well-defined samples ranging from recordable compact discs (CDs) to computer chips.

Another type of probe potentially suitable for the feedback mode imaging is nanopipets.[22a] A pipet can be filled with a solvent immiscible with the outer solution and used as an SECM tip.[22b] The tip current is produced by the transfer of an ion across the liquid/liquid interface [e.g., from water to 1,2-dichloroethane (DCE) inside the pipet]. This current is limited by diffusion of the transferable ion in the outer solution. It decreases when the tip is brought close to a solid substrate, which blocks the diffusion to the pipet orifice (negative feedback). The theory developed for the ion-transfer (IT) feedback mode is similar to the conventional SECM feedback theory, and the quantitative agreement between theoretical and experimental current versus distance curves was demonstrated for nanopipet tips.[22c] Here, we present the first example of high-resolution topographic imaging based on the negative IT feedback.

EXPERIMENTAL SECTION

Chemicals. Ferrocenemethanol ($FcCH_2OH$), LiCl, and KCl purchased from Aldrich and tetraethylammonium chloride (TEACl), chlorotrimethylsilane, and DCE from Sigma were used as received. Solutions of $FcCH_2OH$ and KCl were prepared daily and buffered to pH 4 with 20 mM acetic acid (Baker). Hexaammineruthenium(III) chloride and ammonium hexachloroiridate(IV) were purchased from Strem Chemicals and used without further purification. Ferrocene (Fc; 98%, Aldrich) was sublimed twice. Tetrabutylammonium tetrakis(4-chlorophenyl)borate (TBATPBCl) was prepared by metathesis of KTPBCl and TBACl, as described previously.[23] The ionic liquid, 1-methyl-3-octylimidazolium-bis(tetrafluoromethylsulfonyl)imide ($C_8mimC_1C_1N$), was generously provided by Professor Takashi Kakiuchi (University of Kyoto, Japan). All aqueous solutions were prepared from deionized water (Milli-Q, Millipore Corp.).

Substrate Preparation. Recordable CDs were stripped of their protective layer by dipping them into concentrated nitric acid for several minutes until the layer peeled off completely. This bath also removed the metallic layer from aluminum-coated CDs. CDs were then rinsed with deionized water. Gold CDs were thoroughly cleaned by dipping them in a concentrated ethanol solution of potassium hydroxide for 5 min and then rinsed several times with deionized water. Electronic microcircuits (wafers and microchips) were obtained as a gift from Ms. Mary Westermann (IBM Corporation, East Fishkill, NY). A portion of the wafer that contained the area of interest was carefully cut using a glass cutter and glued to a glass microscope slide.

Electrodes and Electrochemical Cells. Polished Pt working electrodes (50−200 nm radius) were prepared by pulling micrometer-sized Pt wires into a glass capillaries and polishing under video microscopic control and characterized as described previously.[11,21] The overall success rate for the tip preparation is ~80%. A two-electrode setup was used with a 0.25 mm diameter Ag wire coated with AgCl serving as a reference electrode. When $(NH_4)_2IrCl_6$ was used as a redox mediator, a commercial glass-enclosed Ag/AgCl reference electrode was employed to prevent direct contact of Ag with the oxidizing hexachloroiridate(IV) solution. CD substrates were either glued with Torr Seal epoxy (Varian, Lexington, MA) to the bottom of a glass cell or a rectangular glass cell was built on the substrate itself by attaching four pieces of glass slide to it. In some experiments, imaging was carried out in a drop of aqueous solution placed on a hydrophobic substrate surface, and the Ag/AgCl reference electrode was inserted inside the drop. The substrate was secured onto (but kept electrically insulated from) a steel SECM stage with the help of strong magnets.

The nanopipets were made from quartz capillaries (length of 10 cm, o.d./i.d. = 1.0/0.70 mm; Sutter Instrument Co., Novato, CA) using a laser-based pipet puller (P-2000, Sutter Instrument Co.), as described previously.[22] The pipets were filled with organic solution from the rear, using a small (10−25 μL) syringe. A Ag/AgTPBCl ($TPBCl^-$ is tetrakis(4-chloro-phenyl)borate) reference was inserted into each pipet from the rear. The inner glass wall of a pipet was silanized to render it hydrophobic. This was done by dipping the pipet tip into chlorotrimethylsilane for ~5−7 s. This was crucial because the external aqueous solution gets drawn inside a pipet if its inner surface is hydrophilic. Before imaging, the pipet radius was evaluated by steady-state voltammetry and the stability of its response was checked by immersing it into a 0.6 mM aqueous solution of TEACl and passing the diffusion-limiting current of TEA^+ transfer. The pipet was deemed suitable for imaging if the current changed by <3% during 20 min.

SECM Instrument and Procedures. The schematic diagram of our home-built SECM instrument is shown in Figure 1. As described previously,[11] the tip current was measured and its potential was controlled by the EI-400 four-electrode potentiostat (Cypress Systems). The SECM stage was bolted onto a vibration-insulated optical table (Newport).

A National Instrument data acquisition card DT-EZ was installed on a Dimension 9200 (Dell) computer that was used to operate the EI-400 potentiostat. The substrate was always unbiased. The same computer also handled the tip positioning via an 8200 Inchworm motor controller (EXFO-Burleigh) and three motors (TSE-820) with 20 nm resolution optical encoders in a

(17) (a) Mirkin, M. V.; Fan, F.-R. F.; Bard, A. J. *J. Electroanal. Chem.* **1992**, *328*, 47. (b) Slevin, C. J.; Gray, N. J.; MacPherson, J. V.; Webb, M. A.; Unwin, P. R. *Electrochem. Commun.* **1999**, *1*, 282. (c) Kranz, C.; Friedbacher, G.; Mizaikoff, B.; Lugstein, A.; Smoliner, J.; Bertagnolli, E. *Anal. Chem.* **2001**, *732*, 2491.
(18) Macpherson, J. V.; Jones, C. E.; Barker, A. L.; Unwin, P. R. *Anal. Chem.* **2002**, *74*, 1841.
(19) Fan, F.-R. F.; Bard, A. J. *Proc. Natl. Acad. Sci. U.S.A.* **1999**, *96*, 14222.
(20) Macpherson, J. V.; Unwin, P. R. *Anal. Chem.* **2001**, *73*, 550.
(21) (a) Sun, P.; Mirkin, M. V. *Anal. Chem.* **2006**, *78*, 6526. (b) Sun, P.; Mirkin, M. V. *Anal. Chem.* **2007**, *79*, 5809. (c) Velmurugan, J.; Sun, P.; Mirkin, M. V. *J. Phys. Chem. C* **2009**, *113*, 459.
(22) (a) Shao, Y.; Mirkin, M. V. *J. Am. Chem. Soc.* **1997**, *119*, 8103. (b) Shao, Y.; Mirkin, M. V. *J. Phys. Chem. B* **1998**, *102*, 9915. (c) Cai, C.; Tong, Y.; Mirkin, M. V. *J. Phys. Chem. B* **2004**, *108*, 17872.
(23) Shao, Y.; Girault, H. H. *J. Electroanal. Chem.* **1990**, *282*, 59.

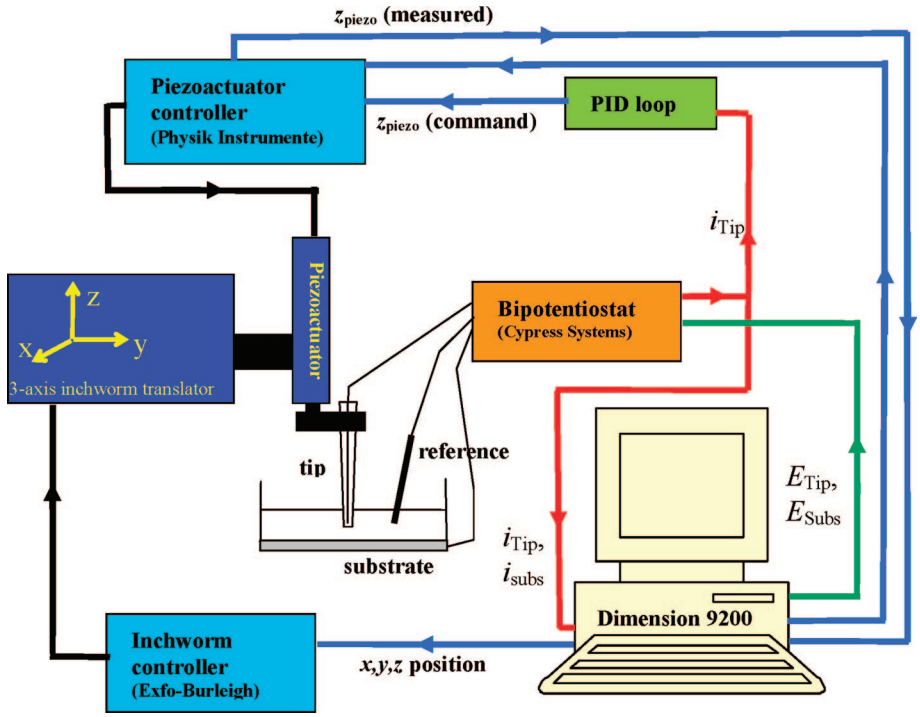

Figure 1. Scheme of the SECM instrument with a feedback PID loop.

closed loop. This configuration was used for constant-height imaging. For higher *z*-axis position resolution (0.1 nm) during constant-current imaging, a PI-843.60 piezoactuator (Physik Instrumente) controlled by an E-500 position controller (Physik Instrumente) was used. The probe was attached to the moving part of the piezoactuator, and the static part of the piezoactuator was fastened onto the 3-D inchworm stage. During constant-current imaging, the computer could read the tip position via the E-500 controller.

A home-built digital proportional−integral−derivative (PID) loop controller using tip current as input signal and tip position as output signal was constructed to control the vertical position of the tip during constant-current imaging. The input signal (i.e., the voltage analog of the tip current) was digitized using a 16 bit analog-to-digital converter (ADS8505, Texas Instruments), then processed with a microcontroller (PIC24HJ256GP610, Microchip), and an output, z_{piezo}, was generated with a 16 bit digital-to-analog converter (DAC8820, Texas Instruments). The output of the PID loop was fed to the analog input of the E-500. The input signal was filtered by summing up a number of samples over a 16.7 ms period (60 Hz). This procedure nearly completely eliminates 60 Hz noise coming from the power line. The bandwidth of the feedback loop was 60 Hz.

To monitor the initial approach of the SECM tip to the substrate, we used binocular lenses focused a few tens of micrometers above the substrate surface. The tip was moved slowly toward the substrate until it appeared in focus. During the final approach, the tip was brought closer to the substrate while monitoring the current, as described previously.[21] All experiments were carried out at room temperature (23 ± 2 °C) inside a Faraday cage.

RESULTS AND DISCUSSION

Imaging Compact Discs in Aqueous Solutions. Once chemically stripped from its protective, metallic, and dye layers, the surface of a rewritable aluminum CD exhibits one spiral groove, which microscopically appears as a series of ~1 μm spaced parallel stripes (Figure 2A). Figure 2B shows an SECM image of a 7 μm × 7 μm portion of CD surface obtained with a 140 nm radius Pt electrode with RG = 10 (RG = rg/a, where rg is the radius of the insulating sheath and a is the Pt disk radius) in a 5 mM ammonium hexachloroirridate(IV) aqueous solution. The tip was scanned in a horizontal plane above the substrate at a scan rate v = 1 μm/s to obtain a constant-height SECM image. The lateral resolution, which is determined by the tip radius[1] (i.e., ~140 nm), was sufficiently high to clearly image the CD surface pattern. A current versus distance curve (Figure 2C) obtained with the same tip approaching the insulating CD surface exhibits negative feedback. The theoretical i_T−d curve in Figure 2C (solid line) was obtained from eq 1[22b]

$$i_T = i_{T,\infty}\left[\left(0..4571825 + \frac{1.4604238}{d/a} + 0.4312735 \exp\left(-\frac{2.350667}{d/a}\right)\right)^{-1} - \frac{0.145437d/a}{5.5768952 + d/a}\right] \quad (1)$$

where $i_{T,\infty}$ is the tip current in the bulk solution (far from the substrate) and a is the tip radius. The experimental curve (symbols) fits the theory for $d \gtrsim 50$ nm and deviates from it at shorter distances. This can be expected because the width of the disk groove is comparable to the tip diameter and its depth is of the order of 50 nm.

Because of the nonlinear relationship between the tip current and the tip/substrate distance (eq 1), the constant-height SECM image does not directly represent the topography of the substrate. With the help of eq 1, the current map shown in Figure 2B was converted to the topographic image (i.e., the dependence of the tip/substrate separation distance versus the tip position). One should note that the tilt angle (~0.7°; the inclination of ~80 nm over a 7 μm distance is due to the imperfect tip/substrate alignment in the y direction) is reversed in Figure 2D as compared

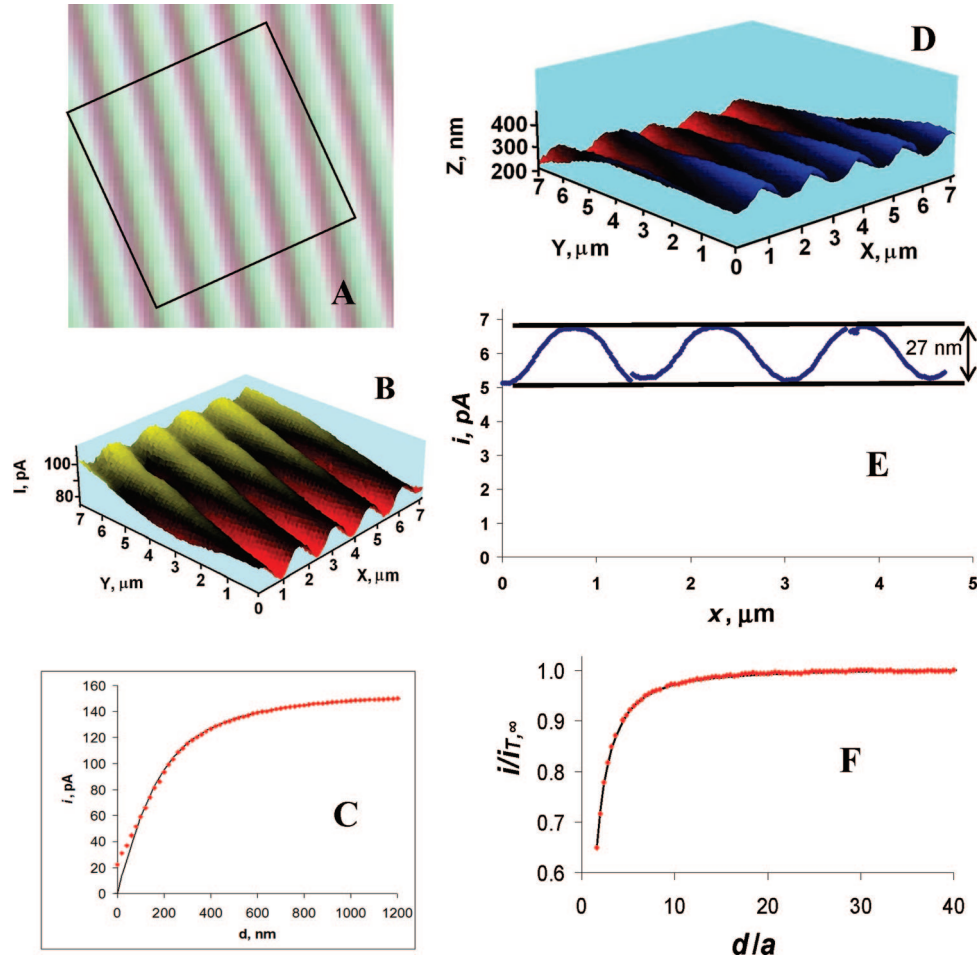

Figure 2. (A) Optical micrograph of CD surface. The 7 μm × 7 μm imaged area is indicated by the black square. (B) SECM image of a 7 μm × 7 μm portion of CD surface obtained with a 140 nm radius Pt electrode. ν = 1 μm/s. (C and F) Experimental (symbols) and theoretical (solid line; computed from eq 1) current−distance curves for 140 nm (C) and 50 nm (F) tips approaching the CD surface. (D) Topographical image remapped from the constant-height SECM image in panel B. (E) Lateral line scan obtained with a 50 nm tip. Small current discontinuities are an artifact caused by piezo clicks. Aqueous solutions contained 250 mM KCl and either 5 mM $(NH_4)_2IrCl_6$ (B−D) or 1 mM $FcCH_2OH$ (E and F). The tip potential was 100 mV (B−D) or 500 mV (E and F) vs Ag/AgCl reference.

to that in Figure 2B. The ridges appearing on the current map (Figure 2B) are also inverted and look like valleys in Figure 2D. The remapped topographic image eliminates the i_T−d nonlinearity so that the ridge/valley distance appears essentially constant over the entire image.

Higher resolution and more detailed topographic information can be obtained by using a smaller tip. A line scan of the same CD (Figure 2E) was obtained with a 50 nm tip. Using the corresponding current−distance curve (Figure 2F) for distance calibration, one can determine the depth of the groove to be 27 nm.

The metallic layer in old rewritable CDs ("gold CDs") was Au rather than Al. The nitric acid treatment in this case strips the protective coating off but leaves a thin gold layer intact. The exposed gold surface was previously used as a platform for sensor fabrication.[24] Figure 3A shows an AFM image of a 5 μm × 5 μm portion of the gold CD surface.[24] The image reveals ~1.2 μm wide plateaus separated by ~300 nm wide valleys. The SECM feedback

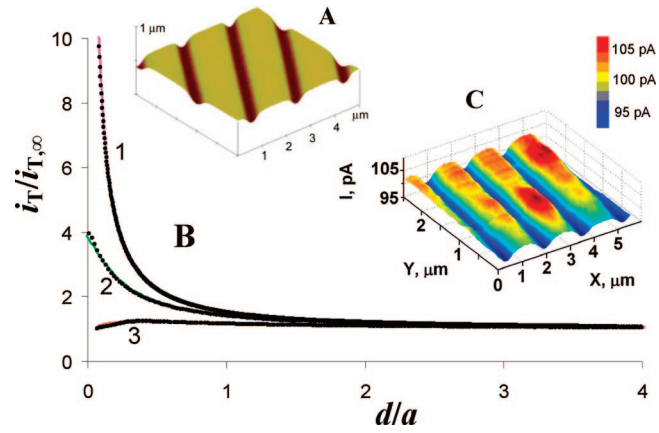

Figure 3. (A) AFM image of a 5 μm × 5 μm portion of Au CD surface (ref 24). (B) Experimental (symbols) and theoretical (ref 25) (solid lines) current−distance curves for different SECM tips approaching a gold CD substrate. The tip radius was 12.5 μm (1), 1 μm (2), and 150 nm (3). (C) Constant-height SECM image of a 2.5 μm × 6 μm portion of gold CD surface obtained with a 140 nm Pt tip. ν = 300 nm/s. (B and C) The solution contained 1 mM $FcCH_2OH$ and 250 mM KCl and was buffered with acetic acid to pH = 4. The tip potential was 500 mV vs Ag/AgCl.

(24) Yu, H.-Z. *Chem. Commun.* **2004**, 2633.

obtained at a gold CD substrate (Figure 3B) is positive due to the electrochemical activity of gold.

The constant-height SECM image of a 2.5 μm × 6 μm portion of the Au CD surface (Figure 3C) was obtained with a 140 nm radius Pt electrode in a 1 mM $FcCH_2OH$ aqueous solution. This image clearly reproduces the plateau/valley surface topography visualized by AFM (Figure 3A). However, on top of the well-defined CD pattern one can see significant local variations in the tip current. These variations could not be caused by topographic features of the CD surface because the nanoscale flatness of Au plateaus is evident from the AFM image. Instead, they are due to the nonuniform electrochemical reactivity of the grainy Au film. Unlike vapor-deposited Au films on glass, whose electrochemical reactivity is uniform and sufficiently high to yield diffusion-controlled SECM feedback at any tip size (e.g., $a \geq 13$ nm[21a]), the finite heterogeneous kinetics can be measured at the gold CD surface using sufficiently small SECM probes. The i_T versus d curves in Figure 3B were obtained with three tips of different radii. With a large tip ($a = 12.5$ μm; curve 1), the process is diffusion-controlled, and the corresponding current−distance curve fits well the theory for the pure positive feedback (solid pink curve calculated from eq 8 in ref 22b). SECM images of gold CDs obtained with a tip of this size (not shown) do not contain any features associated with nonuniform surface reactivity. At a smaller tip (e.g., $a = 1$ μm; curve 2), the higher mass-transfer coefficient[1] results in the mixed diffusion/kinetic control of the mediator regeneration at the substrate, which corresponds to the lower magnitude of the positive feedback. The apparent heterogeneous rate constant found from the fit of the experimental approach curve to the theory (solid green curve calculated from eq 6 in ref 25) was $k = 0.45$ cm/s. A similar rate constant value, $k = 0.50$ cm/s, was obtained with a much smaller tip ($a = 150$ nm; curve 3). This value corresponds to the local rate of the mediator regeneration at the microscopic portion of the CD surface facing the tip electrode. Figure 3C presents a nanoscale map of the electrochemical reactivity.

Imaging in Ionic Liquid. All aforementioned images were obtained in aqueous solutions. However, various applications may require SECM imaging to be done in nonaqueous media, e.g., in ionic liquids whose use as solvents in electrochemical systems is on the rise.[26] Although the SECM has been employed in ionic liquids,[27] a major challenge in imaging experiments is slow diffusion rate in these viscous media. The time required for the diffusion-controlled current flowing at a disk electrode to reach the steady state can be roughly estimated as $t_{ss} \cong 50a^2/D$,[28] where D is the diffusion coefficient of redox species in solution. In an aqueous solution, D is ~10^{-5} cm^2/s, and t_{ss} is ~0.05 s for a 1 μm radius tip. Such a tip can be scanned over the substrate surface at a reasonably high speed (a few micrometers per second) without significant deviations from the steady state. In contrast a typical D value in a moderately viscous ionic liquid (like $C_8mimC_1C_1N$ used in our experiments) is ~10^{-7} cm^2/s, and so $t_{ss} \sim 5$ s (for a 1 μm radius tip) is too large for feedback mode SECM imaging. This problem can be overcome by using smaller tips; e.g., under the same experimental conditions, t_{ss} is ~0.05 s for $a = 100$ nm. Figure 4 shows a constant-height SECM image obtained with a 190 nm Pt tip in $C_8mimC_1C_1N$ containing 50 mM Fc. $v = 500$ nm/s is within the range of scan rates employed for imaging in aqueous solutions (cf. Figures 2B and 3C). The surface pattern is essentially identical to that in Figure 3 demonstrating that high viscosity of $C_8mimC_1C_1N$ does not affect the SECM image. A portion of the CD surface imaged in Figure 4 exhibited relatively uniform reactivity—only minor variations can be detected. In other images obtained in $C_8mimC_1C_1N$ (not shown), larger local variations in surface reactivity were evident.

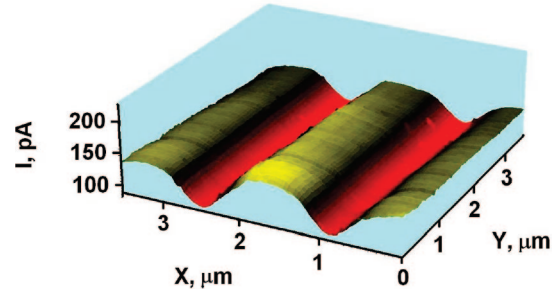

Figure 4. Constant-height SECM image of the 3.5 μm × 3.5 μm portion of the gold CD surface obtained with a 190 nm Pt tip in ionic liquid. The $C_8mimC_1C_1N$ solution contained 50 mM Fc. The lateral scan rate was 500 nm/s.

Microcircuit Imaging. Microcircuits are generally built on silicon wafers by locally diffusing doping species, selectively etching parts of the wafer, and electrodepositing copper or aluminum interconnects. Computer microchips and wafers possessing very rough surfaces with small, sharp features are much harder to image than CDs whose surfaces exhibits relatively flat, regular patterns. The first microcircuit substrate used in our imaging experiments was an erasable programmable read-only memory (EPROM) of a Motorola 68HC05 chip containing micrometer-sized features. To match an SECM image with an optical picture of the substrate, one has to obtain an electrochemical map of a relatively large (i.e., tens of micrometers) area. Constant-height imaging of a large area with a nanotip scanned laterally in the $x-y$ plane above the substrate is not straightforward because of the practically unavoidable small (e.g., ~0.7° in Figure 2B) tip/substrate misalignment. If the lateral scan length is incomparably larger than a, the tip/substrate separation distance changes significantly, and the tip is likely to hit one of the taller surface features of the microcircuit. By keeping the tip current constant (constant-current mode; if the feedback is either pure positive or negative, d remains essentially constant for the entire image[15b,16]) one can reduce the chances of the tip crash.

Figure 5 shows an optical image of the EPROM of a Motorola 68HC05 chip (A) and a constant-current SECM image of the 57 μm × 57 μm portion of the same area (B). The constant-current SECM image was acquired in a 1 mM aqueous solution of $FcCH_2OH$ with a 100 nm Pt tip held ~200 nm away from the

(25) Wei, C.; Bard, A. J.; Mirkin, M. V. *J. Phys. Chem.* **1995**, *99*, 16033.
(26) (a) MacFarlane, D. R.; Forsyth, M.; Howlett, P. C.; Pringle, J. M.; Sun, J.; Annat, G.; Neil, W.; Izgorodina, E. I. *Acc. Chem. Res.* **2007**, *40*, 1165. (b) Hapiot, P.; Lagrost, C. *Chem. Rev.* **2008**, *108*, 2238.
(27) (a) Laforge, F. O.; Kakiuchi, T.; Shigematsu, F.; Mirkin, M. V. *J. Am. Chem. Soc.* **2004**, *126*, 15380. (b) Carano, M.; Bond, A. M. *Aust. J. Chem.* **2007**, *60*, 29. (c) Ghilane, J.; Lagrost, C.; Hapiot, P. *Anal. Chem.* **2007**, *79*, 7383. (d) Taylor, A. W.; Qiu, F.; Hu, J.; Licence, P.; Walsh, D. A. *J. Phys. Chem. B* **2008**, *112*, 13292.
(28) (a) Wightman, R. M.; Wipf, D. O. In *Electroanalytical Chemistry*; Bard, A. J., Ed.; Marcel Dekker: New York, 1989; Vol. 15, p 267. (b) Amatore, C. In *Physical Electrochemistry: Principles, Methods, and Applications*; Rubinstein, I., Ed.; Marcel Dekker: New York, 1995; p 131.

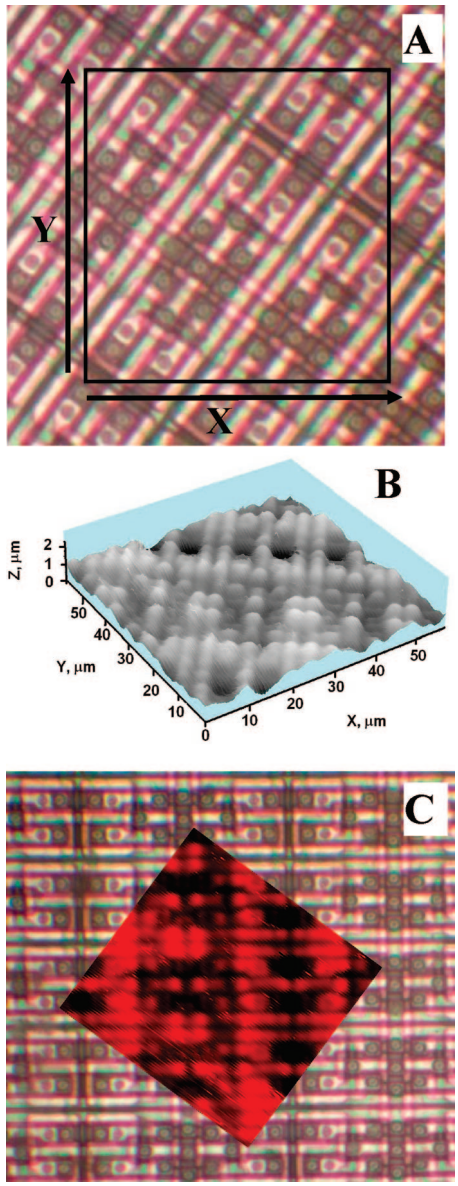

Figure 5. Optical image of the EPROM of the Motorola 68HC05 chip (A) and constant-current SECM image (B) of the 57 μm × 57 μm area delimited by the black square in panel A. The SECM image was obtained in 1 mM $FcCH_2OH$ aqueous solution with a 100 nm Pt tip. The tip/substrate distance was ~200 nm, and the current was set at 21 pA (70% or the bulk value). The imaging time was 20 min at the 3 μm/s scan rate. (C) The SECM image (panel B) superimposed on the optical micrograph (panel A). Both pictures were rotated to ensure their proper orientation.

surface. An external digital feedback control loop was implemented to maintain the constant i_T value during the $x-y$ scan (see the Experimental Section). The output signal from the E-500 piezo controller was used to monitor the absolute z-axis tip position. A constant-distance SECM image is therefore a direct picture of the substrate topography. The substrate surface exhibits a maximum height differential of ~2 μm, which corresponds to ~20 times the tip radius; therefore, this image could not have been obtained in a constant-height mode without crashing the tip.

An unambiguous verification of a chip pattern produced by SECM was obtained by superimposing it on the optical micrograph (Figure 5C). A very close correspondence can be seen between micrometer-sized features in the optical and electrochemical images. The lateral resolution that can be obtained with an SECM nanotip is higher than that attainable in conventional optical microscopy (i.e., ~0.5 μm). This cannot be seen in Figure 5 because the smallest EPROM feature is greater than 1 μm. We used IBM wafers built with the 90 nm process technology as a "real-world" sample with a smaller feature size. Figure 6A shows an optical image of an electroinactive area of the wafer located inside a microcircuit. Figure 6B is a 12 μm × 12 μm constant-height SECM image of the region delimited by the black rectangle that was obtained with a 55 nm Pt tip. The electrochemical image reproduces well the features discernible on the optical image. The small size of the tip allowed us to zoom in onto a 3.5 μm × 3.5 μm portion of the surface (Figure 6C) represented by the blue square in Figure 6B.

A potentially useful application of high-resolution SECM imaging is to detect small defects in the wafers. Figure 7A shows an optical micrograph of an electroinactive region separating microcircuits on the wafer. A microscopic defect appears as a faint pinkish spot in the lower left corner of the image area delimited by the black rectangle. The geometric pattern of the wafer surface (i.e., a square array of submicrometer-sized, pyramidal bumps) is completely intact in the defect area. A 9 μm × 8 μm constant-current SECM image (Figure 7B) corresponding to the black rectangle area in Figure 7A shows a square pattern in accordance with the optical image. A striking difference is that Figure 7B exhibits a large "dip" in the area corresponding to a barely visible defect in Figure 7A. Clearly, this "dip" is not a topographic feature (such a feature would have been visible in Figure 7A) but a spot of increased surface reactivity. Unlike the rest of the surface, which exhibits pure negative feedback, some regeneration of the redox mediator occurs at this spot and produces a diplike feature in the constant-current SECM image (i.e., the tip is moved closer to the surface to maintain the set current value).

Imaging with Nanopipet Tips. Figure 8 shows a 1.8 μm × 1.8 μm constant-height image of the etched wafer region similar to that pictured in Figure 7. This image was obtained using a nanopipet probe filled with DCE solution containing TBATPBCl electrolyte. The tip current was produced by the transfer of TEA^+ from the external aqueous solution to DCE. The tip potential was held at −400 mV versus aqueous Ag/AgCl reference, at which the TEA^+ transfer occurred at a diffusion-controlled rate. The pipet radius (a = 106 nm) was determined from the steady-state voltammogram assuming RG = 1.5.[22b,c] The surface pattern in Figure 7A is in agreement with the optical micrograph (Figure 7A) and a constant-current SECM image obtained with a Pt tip (Figure 7B). An advantage of a sharp nanopipet probe over a conventional SECM tip is in very small RG, which makes it easier to image nonflat surface features without crashing the tip. However, the magnitude of the negative IT feedback (i.e., the decrease in the tip current at the given value of the normalized separation distance, d/a) is lower for a pipet than for a conventional probe with a larger RG because of the TEA^+ diffusion from the back of the tip.[22b] Therefore, a pipet has to be brought closer to the substrate surface to attain the same magnitude of the negative feedback.

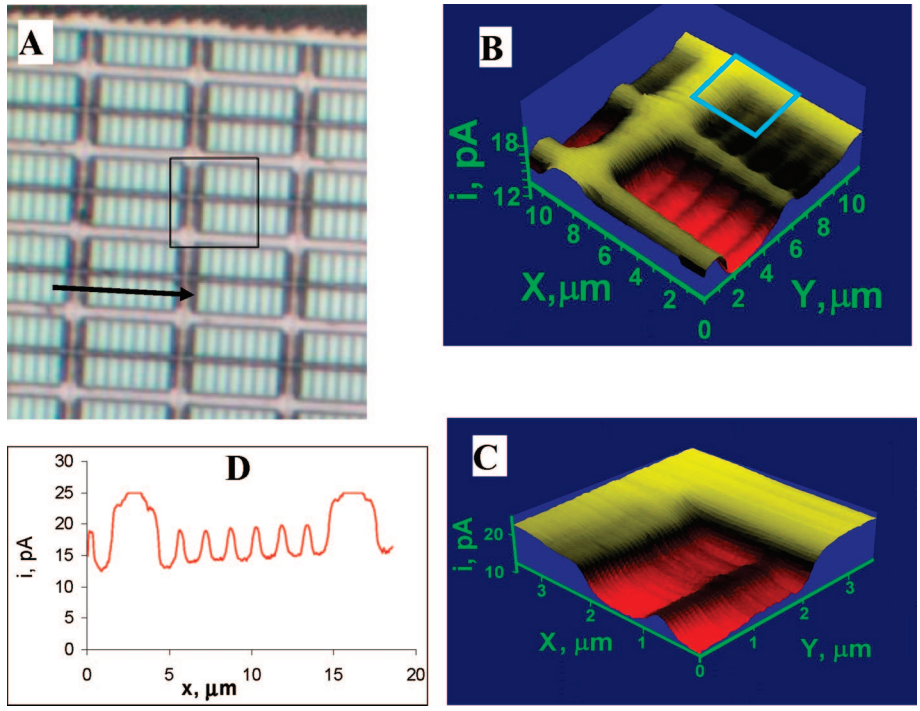

Figure 6. Optical (A) and SECM (B–D) images of an IBM wafer. (B) Constant-height SECM image of the 12 μm × 12 μm area delimited by a black square in panel A. (C) 3.5 μm × 3.5 μm constant-height image of the area marked by the blue square in panel B. (D) Lateral line scan of the tip over the wafer surface shown by the arrow in panel A. The aqueous solution contained 250 mM KCl and 1 mM $FcCH_2OH$. $a = 55$ nm. $\nu = 600$ nm/s (B) and 200 nm/s (C).

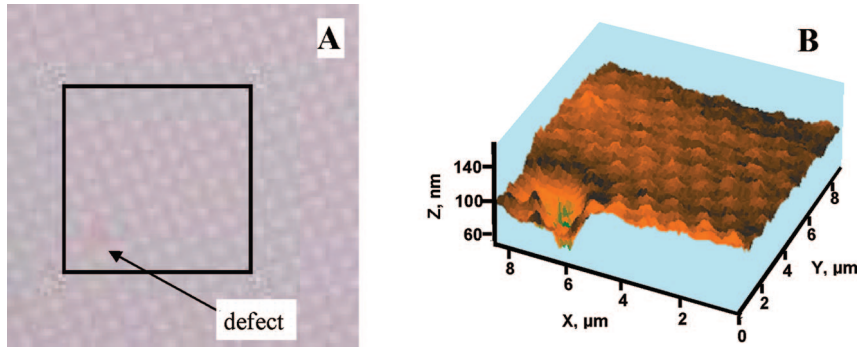

Figure 7. (A) Optical image of an IBM wafer showing a microscopic defect and (B) constant-current SECM image of the 9 μm × 8 μm region delimited by the black rectangle in panel A. The solution contained 5 mM $Ru(NH_3)_6Cl_3$ and 250 mM KCl. $a = 190$ nm. $\nu = 500$ nm/s.

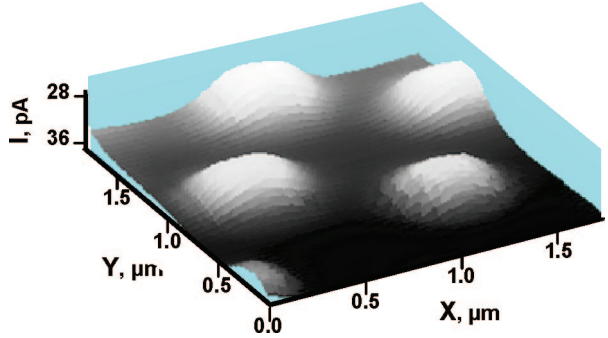

Figure 8. Constant-height IT SECM image of the 1.8 μm × 1.8 μm portion of an IBM wafer obtained with a 106 nm radius pipet-based tip in aqueous solution containing 0.6 mM TEACl and 10 mM LiCl. The filling DCE solution contained 10 mM TBATPBCl. $\nu = 200$ nm/s.

It is interesting to compare ion-transfer-based SECM imaging to a somewhat related technique—scanning ion conductance microscopy (SICM)—in which a nanopipet is used as a scanning conductivity probe.[29] In SICM, a significantly higher tip current and the absence of the liquid/liquid interface result in a more robust imaging procedure and slightly higher lateral resolution (~10–20 nm). The advantage of the IT-based SECM is in its chemical specificity. Since the tip current is produced by the transfer of one specific ion (e.g., TEA^+), SECM can be used for studying IT reactions,[22c] e.g., ion transfers across biological and artificial membranes. Interfacial IT rates can be mapped in addition to topographic imaging discussed in this paper.

CONCLUSIONS

We have demonstrated that different modes of the SECM operation can be used to image surface topography on the

(29) (a) Hansma, P. K.; Drake, B.; Marti, O.; Gould, S. A. C.; Prater, C. B. *Science* **1989**, *243*, 641. (b) Korchev, Y. E.; Bashford, C. L.; Milovanovic, M.; Vodyanoy, I.; Lab, M. J. *Biophys. J.* **1997**, *7*, 653.

nanoscale. Since the spatial resolution of the SECM is governed by the tip radius, the use of nanometer-sized probes allows one to attain the lateral resolution in the range of tens of nanometers. The smallest feature size in the employed samples (~200 nm) was significantly larger than the spatial resolution attainable with our smallest tips. The ultimate limit for the lateral resolution of SECM should be ~5 to 10 nm, whereas the *z*-axis resolution can be as high as ≤1 nm.[21a] An additional advantage of nanometer-sized amperometric probes is the fast mass transfer, which allows SECM imaging to be done under steady-state conditions in viscous media such as ionic liquids.

Unlike previous studies, where submicrometer-sized SECM probes were employed to image soft substrates (e.g., biological cells[11] or liquid-filled pores[18]), here we imaged "real-world" solid samples with irregular surface features, e.g., electronic microcircuits, without tip/substrate collisions that would have resulted in tip crashes. This was possible in part because of the well-defined geometry of our flat, polished tips, which allowed accurate evaluation of *d* from the tip current. The constant-current mode of the SECM imaging was especially useful for acquiring images of large areas of nonflat and tilted substrates.

Another advantage of well-characterized disk-type nanotips is the possibility of quantitative data analysis. In the case of either pure positive or negative feedback, the obtained current map can be converted to the topographic image, as it was done in Figure 2D. If the tip current is limited by finite rate of mediator regeneration at the substrate, SECM can be used for nanoscale mapping of surface reactivity, and local heterogeneous kinetics can be determined from the current versus distance curves. Nanopipet-based probes, which we used for topographic imaging, should also be suitable for nanoscale mapping of ionic conductance of biological and artificial membranes.

ACKNOWLEDGMENT

The support of this work by the National Science Foundation (CHE-0645958) and a Grant from PSC−CUNY are gratefully acknowledged. We thank Professor Takashi Kakiuchi (Kyoto University) for generously providing $C_8mimC_1C_1N$ ionic liquid and James Carpino for his help with building our SECM instrument. We are indebted to Ms. Mary Westermann and Dr. Richard Hoffman for IBM wafers and microchips used in our experiments.

Received for review February 12, 2009. Accepted February 20, 2009.

AC900335C